1 Introduction and Overview

1.1 Executive Summary

Current and upcoming neutrino oscillation experiments in the United States, Europe and Japan have driven the construction of new, very intense neutrino beamlines required to achieve reasonable event rates at detectors located hundreds of kilometers away. These new beamlines allow us to initiate a vigorous neutrino scattering research program at a detector, located close to the production target, where event rates are much higher than at the previous generation of neutrino beam facilities. Note, furthermore, that it is neutrino oscillation experiments, with their low-energy neutrinos and massive nuclear targets, which highlight the need for much improved knowledge of low-energy neutrino-Nucleus interactions.

At Fermilab, the NuMI beam, designed for the MINOS neutrino oscillation experiment, yields several orders of magnitude more events per kg of detector per year of exposure than the higher-energy Tevatron neutrino beam. With this much-increased intensity, one can now perform statistically-significant neutrino scattering experiments with much lighter targets than the massive iron, marble and other high-A detector materials used in the past. That these facilities are designed to study neutrino oscillations points out the second advantage of these neutrino scattering experiments: An excellent knowledge of the neutrino beam will be required to reduce the beam-associated systematic uncertainties of the oscillation result. This knowledge of the neutrino spectrum will also reduce the beam systematics in the measurement of neutrino-scattering phenomena.

The MINERνA experiment (Main INjector ExpeRiment: ν-A), a collaboration of elementary particle and nuclear physics groups and institutions, will run in the NuMI beamline, and be sited in the hall which currently houses the MINOS near detector. With considerable available space, the hall is an ideal environment for neutrino experiments. It provides a well-shielded area with sufficient infrastructure to support MINERνA as well as MINOS.

MINERνA will complete a physics program of high rate studies of exclusive final states in neutrino scattering including quasi-elastic scattering, and resonant and coherent pion production. MINERνA will also study the poorly understood transition region between non-perturbative and perturbative QCD in the higher mass resonance region and the application of duality with the weak current. MINERνA will contribute significantly to the study of parton distribution functions (PDFs) in the poorly known high-x_{Bj} region as well as quark-flavor dependent studies of generalized parton distributions (GPDs). Studies on several nuclear targets will explore nuclear effects, another topic that has not been studied with neutrinos up to now, and will bring important constraints to determining nuclear PDFs.

MINERνA results will also be very important for present and future neutrino oscillation experiments, where the details of neutrino cross-sections and final states as well as nuclear effects are essential in determining the energy of the incoming neutrino and in separating backgrounds to oscillation from signal.

MINERνA will address all these topics with a comparatively simple, high-precision detector composed of several sub-detectors with distinct functions in reconstructing neutrino inteactions. The target volume (approximately 6 tons) for most analyses is the inner “Totally Active Detector” where the only material is the sensitive scintillator strips themselves. The scintillator detector does not fully contain events due to its low density and lowZ, so the MINERνA design surrounds it with sampling detectors; electromagnetic and hadronic calorimeters. The nuclear targets of graphite, iron and lead will be located in the upstream end of the detector.

1.2 The NuMI Near Detector Hall

The NuMI Near Detector Hall[1] is a fully-outfitted experimental facility that can accomodate MINERνA with a limited number of additions to the infrastructure.

The hall is 45 m long, 9.5 m wide, 9.6 m high, with its upstream end just over 1 km from the NuMI target, at a depth of 106 m below grade. The MINOS near detector has been installed at the downstream end of the hall, and there is free space upstream amounting to, roughly, a cylinder 26 m in length and 3 m in radius. The neutrino beam centerline descends at a slope of $3.3°$ and enters the MINOS detector at a height of 3 m from the floor.

Ground water is pumped from the NuMI/MINOS complex at a rate of approximately 200 gallons (750 l) per minute. The hall floors and walls are occasionally damp in places, and a drip cover will be used to protect MINERνA from moisture. The air is held at a temperature between $60°$ F and $70°$ F ($15°$ C and $21°$ C), and 60% relative humidity.

1.2.1 Utilities

The MINOS Service Building on the surface houses the access shaft to the Near Detector Hall and is the entry point for electrical, cooling, and data services to the hall. A 15-ton capacity crane, with a hook height of 18.5 feet (5.66 m), was used to lower the 3.47 ton MINOS detector planes to the hall. MINOS planes were moved within the hall using an overhead 15-ton crane, with 22 foot (6.7 m) hook height and a coverage along the beam axis of approximately 40 m. The procedure for installing MINERνA will closely follow that used by MINOS.

Quiet power to the hall is provided by a 750 KVA transformer at the surface, which branches to a 45 KVA transformer for the muon monitoring alcoves, and two 75 KVA transformers for the Near Detector hall. The power needs of the MINOS detector account for the capacity of the 4 panelboards served by the two 75 KVA transformers. The estimated power consumption of MINERνA's electronics is around 5000 W. MINERνA will require an additional 75 KVA transformer as well as additional panelboards. Both the transformer and panelboards have already been installed by Fermilab.

The heat sink for the MINOS LCW cooling circuit is the flux of ground water collected in the MINOS sump. This cooling is adequate for MINOS, ¡with an output water temperature of $70°$ F. The relatively low heat load of the MINERνA electronics will be absorbed without problem by the MINOS hall air conditioning.

1.2.2 Detector placement

The downstream face of the last MINERνA plane will be placed 2.0 m upstream of the upstream face of the first MINOS plane as shown in Figure 2. This will leave sufficient work space between the two detectors and will avoid interfering with the MINOS coil, which extends approximately 1.7 m upstream of MINOS, to the lower right in the view of Figures 1 and 3. To have the beam axis intersect the detector axis close to the center of the active plastic target, the lowest corner of MINERνA will be placed 1.10 m above the hall floor. The beam centerline will enter the detector at an elevation of 3.4 m from the floor.

1.2.3 Impact on MINOS

The impact of MINERνA on the MINOS installation has been and will continue to be minor. The power supply for the MINOS coil had to be moved upstream and the stairway accessing the upper MINOS electronics racks had to be moved. The drip-ceiling covering the MINOS experiment will be extended to also cover MINERνA during an upcoming Fermilab shutdown.

The presence of the detector in the neutrino beam will cause an increase in the rate of activity in the MINOS detector, mainly in the first (upstream) 20 planes forming the MINOS veto region. Given MINERνA's total mass of $\approx$ 200 tons, for the majority running of the MINOS experiment that uses the lowest energy NuMI beam tune, the expected event rate in the detector is $\approx$ 1.2 charged-current interactions per 10^{13} protons on target (POT). For a spill of 2.5×10^{13} POT this corresponds to 3.0 charged-current events, plus an additional 1.0 neutral-current event per spill. Combining the excellent timing resolution of both MINERνA and MINOS with the fact that the vectors of all particles leaving MINERνA with a trajectory heading towards MINOS will be made available when MINERνA is taking data, this rate should be easily managable. Even when running the NuMI beam in the higher energy (ME) tune, the increase in rate should be $\approx$ 3.5, and that is still managable.

1.3 The NuMI Beam and MINERνA Event Sample

The NuMI neutrino beam is produced from π- and K-decay in a 675 m decay pipe beginning 50 m downstream of the graphite target that is followed by a double horn focusing system. At the end of the decay pipe a 10 m long hadron absorber stops the undecayed secondaries and non-interacting primary protons. Just downstream of the absorber, 240 m of Dolomite is used to range out muons before the ν beam enters the Near Detector Hall. Figure 4 shows the beamline and layout.

1.3.1 Energy options

The neutrino energy spectrum of the NuMI beam can be adjusted by changing the distances of the target and second horn with respect to the first (fixed) horn, as in a zoom lens. The three standard configurations result in three beam energy tunes for the low- (LE), medium- (ME), and high-energy (HE) ranges respectively. However, to switch from one beam mode to another requires down-time, to reconfigure the target hall, and a consequent loss of beam time. An alternative procedure, which also allows the peak energy to be varied, is to change the distance of target from the first horn and leave the second horn fixed in the LE position. Although the resulting event rates are lower in comparison with those involving the movement of the second horn (ME and HE), the movement of the LE target can be accomplished remotely and quickly with a maximum target excursion of -2.5 m upstream of the first horn from its nominal low-energy position. Moving the target -1.0 m results in a "semi-medium" energy beam tune (sME), and -2.5 m produces a "semi-high" energy beam (sHE). A considerably more efficient sHE beam is possible with three-day downtime to move the target to its normal HE

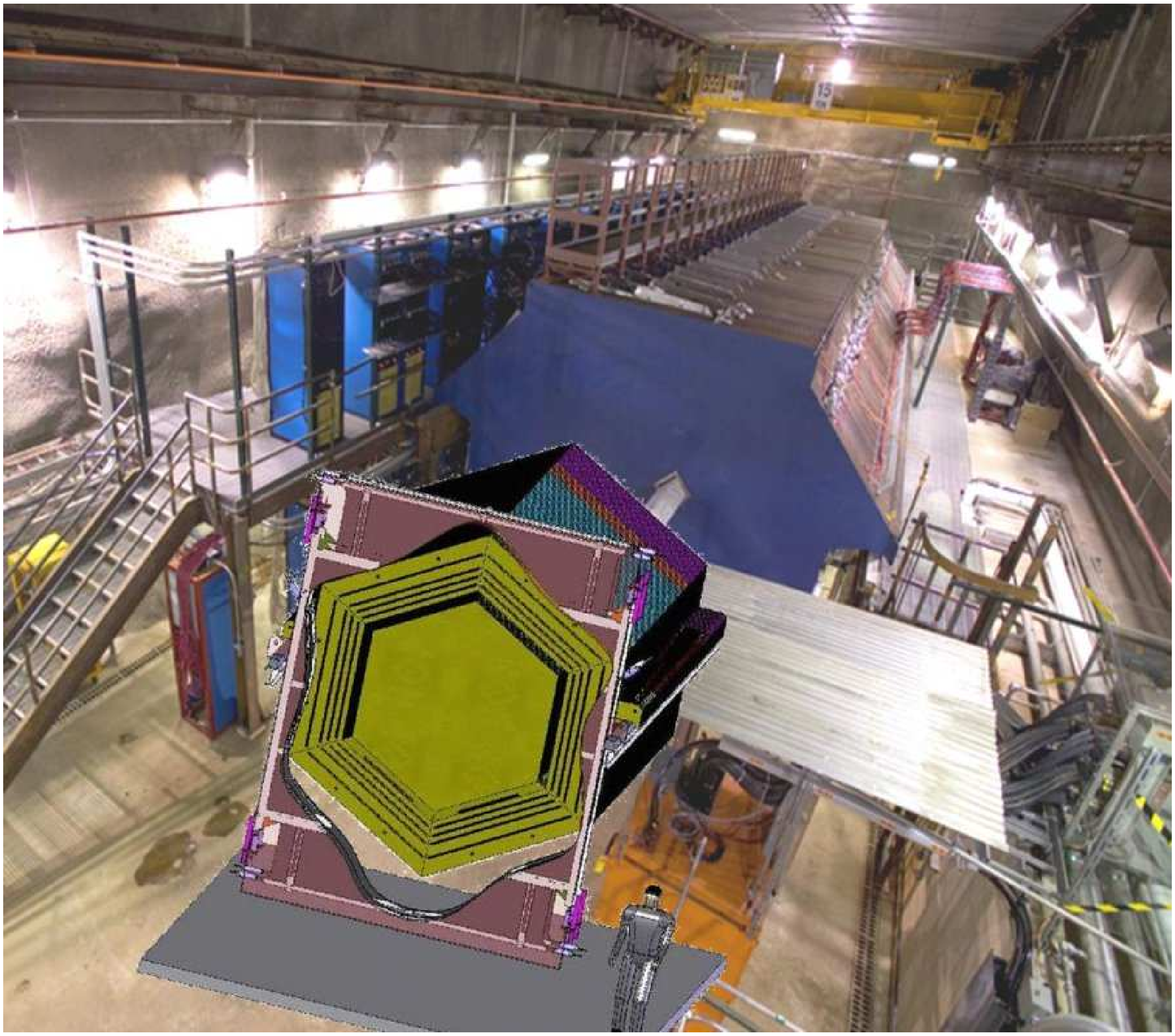

Figure 1: Isometric engineering concept of the proposed MINERνA detector in its home in the NuMI near hall. The photo looks downstream to the MINOS near detector.

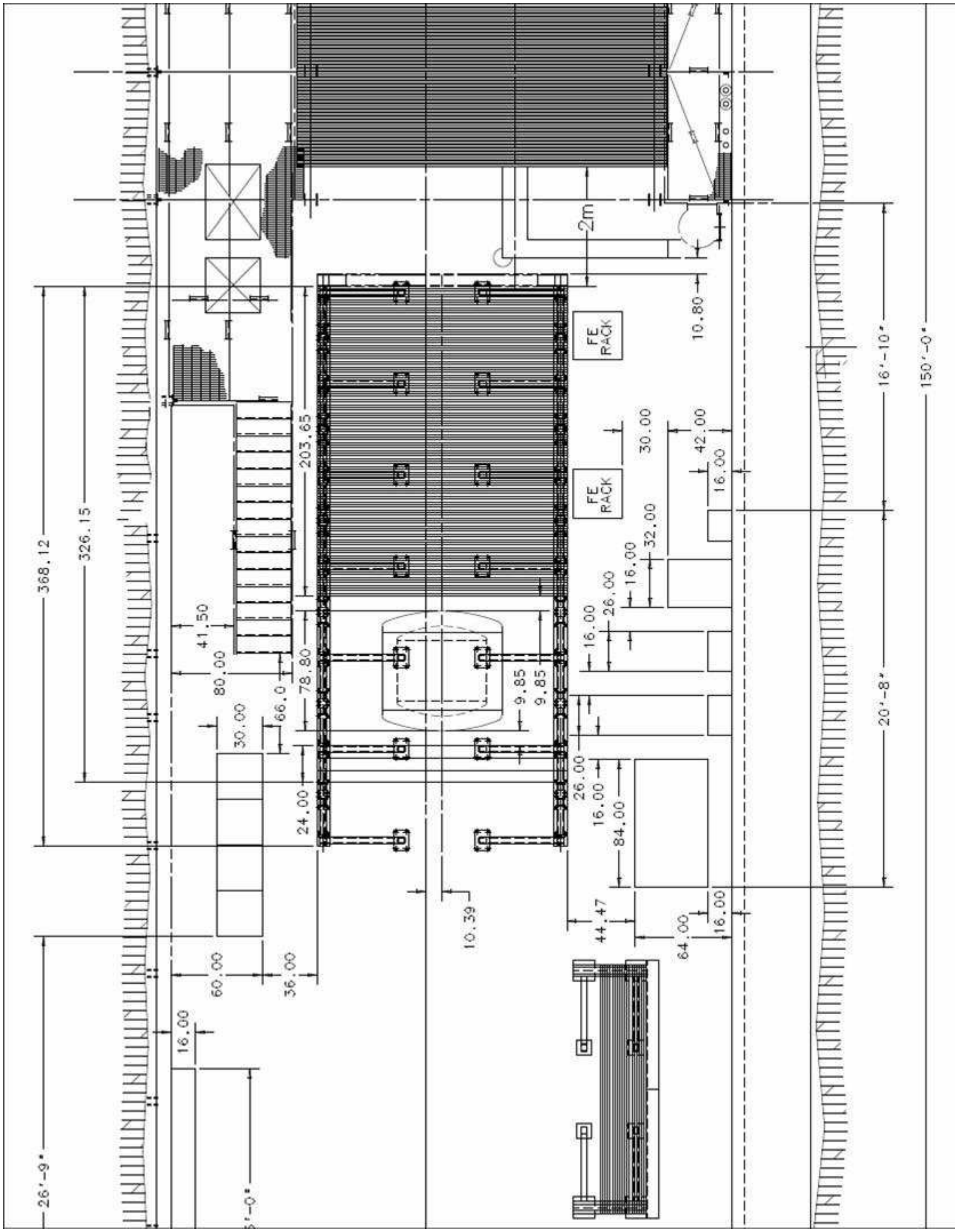

Figure 2: Plan view of MINERνA in the NuMI near hall

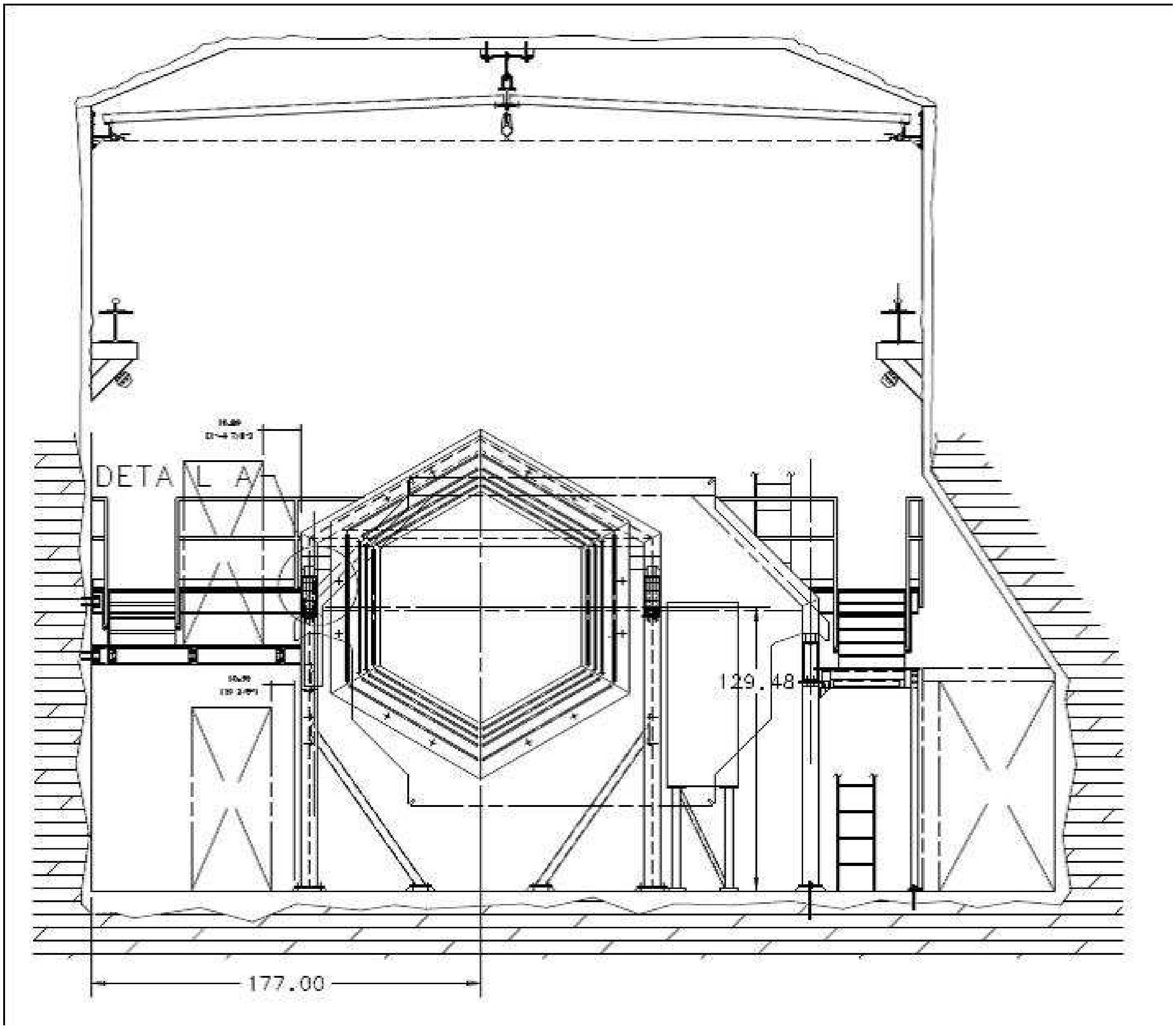

Figure 3: Front view of MINERνA in the NuMI near hall

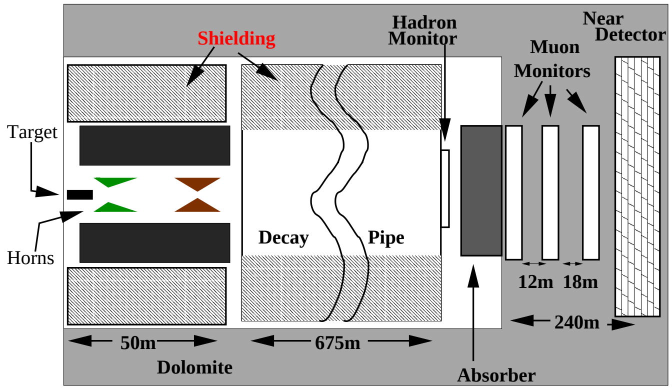

Figure 4: Layout of NuMI beamline components and near detector hall (not to scale).

position of -4.0 m. This more efficient sHE(-4.0) beam would yield over 50% more events than the sHE(-2.5) beam.

When MINERνA is running parasitically with MINOS, the beamline will be operating primarily at its lowest possible (LE) neutrino energy setting, to reach the lowest values of Δm^2. However, to minimize systematics, MINOS will also run in the sME and sHE configurations. The neutrino energy distributions for the LE, sME, and sHE running modes are shown in Figure 5.

When MINERνA is running parasitically with NOνA the beamline will be operating in the medium energy - ME- configuration.

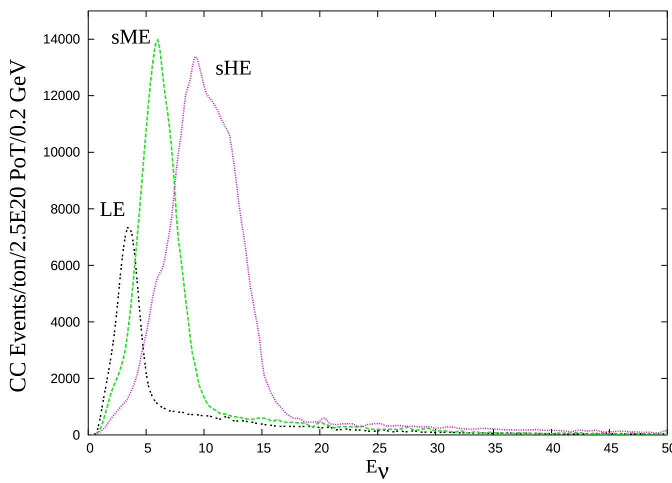

Figure 5: Neutrino energy distribution for charged-current interactions in three configurations of the NuMI beam corresponding to low-energy (LE), medium-energy (sME) and high-energy (sHE).

1.3.2 MINERνA event rates

Table 1 shows charged-current interaction rates per 10^{20} protons on target (PoT) per ton for different neutrino beam energy configurations.

Beam	CC ν_μ
LE	60 K
ME	235 K
sME	132 K
sHE	212 K

Table 1: MINERνA charged-current interactions per ton, per 10^{20} protons on target.

The same beam configurations with horn-currents reversed focus π^- to create anti-neutrino beams. The $\overline{\nu}_\mu$ charged-current interactions from anti-neutrino configurations (LErev, MErev, and HErev) are of great interest and would be highly desirable for MINERνA's physics program. Table 2 shows charged-current anti-neutrino interaction rates per 10^{20} protons on target (PoT) per ton for different neutrino beam energy configurations.

Beam	CC $\overline{\nu}_\mu$	CC ν_μ
LErev	26 K	34 K
MErev	56 K	10 K
HErev	75 K	13 K

Table 2: MINERνA charged-current $\overline{\nu}_\mu$ interactions per ton, per 10^{20} protons on target.

The baseline MINERνA four-year run plan assumes one year running parasitically with MINOS in the LE beam and 3 years running parasitically with NOνA in the ME beam. The assumed protons-on-target for each of the four years is 4×10^{20} PoT. With this 4-year run plan, the total expected charged current event rate is $\approx$ 2.9 million per ton of detector and the event rates per ton for each CC physics-channel is shown in Table 3. As will be described in detail in the MINERνA Project section of this report, the fiducial volume of the fully-active central detector will be 3 tons while the fiducial volume of the nuclear targets will be 0.14 ton, 0.69 ton and 0.86 ton for C, Fe and Pb respectively.

Process	CC/ton	NC/ton
Quasi-Elastic	270 K	90 K
Resonance	530 K	165 K
Transition	670 K	210 K
DIS	1370 K	400 K
Coherent	28 K	14 K
Total (ν)	2870 K	880 K

Table 3: MINERνA samples per ton for various processes assuming the 4-year run plan described in the text.

Required Statistics using the NuMI Low-energy (LE) Beam Configuration For the given distance between Fermilab and the MINOS or NOνA far detectors in northern Minnesota, the expected neutrino oscillation maximum is between 1 and 2 GeV. The neutrino energy region up to 3 GeV, that brackets oscillation maximum, is therefore crucial to both MINOS and NOνA. As shown in Figure 6, to maximize statistics in this region, the MINOS collaboration chose to run with the LE beam for the obvious benefit of extending the reach of the experiment to the lowest values of Δm^2. Although NOνA has chosen to run with the ME configuration, it is running with the far detector in an off-axis position so that the energy of neutrinos reaching their far detector is considerably lower than the on-axis spectrum and falls in the crucial $\leq$ 3 GeV region. It is then in this $\leq$ 3 GeV neutrino energy region that MINERνA must have the statistical precision to precisely measure cross sections and nuclear effects to optimally help MINOS and NOνA minimize their systematic errors.

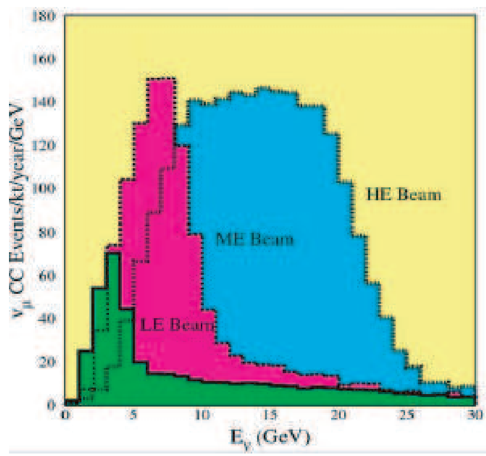

Figure 6: Neutrino energy distribution for charged-current interactions in three configurations of the NuMI beam corresponding to the on-axis low-energy (LE) , full medium-energy (ME) and full high-energy (HE) configurations.

The comparison between the LE and ME beams shown in Figure 6 clearly demonstrates that the LE beam delivers considerably more neutrino events per POT in this crucial energy raange. Table 4 indicates quantitatively the superiority of the LE beam in delivering low-energy neutrino events.

Energy Bin	Ratio: LE to ME Events
0 - 1 GeV	8.0
1 - 2 GeV	3.25
2 - 3 GeV	1.5

Table 4: Expected ratio of events per POT using the NuMI LE compared to ME beam configurations in the energy bins between 0 and 3 GeV

If we change the baseline MINERνA four-year run plan to assume no running in the LE beam and 4 years running parasitically with NOνA in the ME beam (4×10^{20} PoT/year), the loss of statistics in the crucial neutrino energy bins is summarized in table 5.

Energy Bin	Fraction of Events Lost
0 - 1 GeV	0.65
1 - 2 GeV	0.4
2 - 3 GeV	0.15

Table 5: Expected loss of events with a 4-year ME beam run compared to a 1-year LE + 3-year ME beam run.

This loss of statistics on an absolute scale is sufficient to reduce the number of events, for example, in the study of the contentious low-energy behavior (0 - 2 GeV) of CC coherent pion production from 500 to just over 200 events. This will compromise the statistical weight of MINERνA's ability to compare with the recent surprising K2K result [10] and to distinguish between competing models in this energy region. The effect of this loss of statistics in the low-energy region is being studied quantitatively for other channels including quasi-elastic, resonant 1-π production, nuclear effects and the ν_e analysis.

1.3.3 Precision of neutrino flux prediction

In addition to huge event rates, one of MINERνA's significant advantages over previous wide-band neutrino scattering experiments will be better knowledge of the neutrino flux and energy spectrum. Since the NuMI beamline is designed for the MINOS oscillation experiment, considerable effort has been devoted to control of beam-related systematic uncertainties.

The largest source of uncertainty in the neutrino energy spectrum arises from the hadron ($\pi^{\pm}$ and K) prodution spectra. To reduce this uncertainty, a dedicated Fermilab experiment called MIPP (E-907)[7, 4] is directly measuring these hadron production spectra for various nuclear targets. One of the E-907 measurements has been to expose the actual NuMI LE target to the 120 GeV Main Injector proton beam. Using the NuMI target material and shape, E-907's data will include secondary and tertiary hadron production, which significantly modifies the spectra relevant for neutrino production. With input from E-907, the bin-to-bin energy spectrum should be known to $\approx$ 2% and the absolute neutrino flux should be known to $\approx$ 5%.

For the absolute flux of neutrinos, a second uncertainty concerns the number of protons on target. With the current NuMI primary proton beamline instrumentation[8], the number of protons on target will be known to within (1 - 1.5)%, the range being determined by control of the drift in the proton beam toroid devices.

Flux uncertainty estimates Figure 7 shows the level of flux precision at present (without input from the MIPP experiment), for the LE and ME beam configurations (from MINOS) [11].

The impact that these flux uncertainties will have on MINERνA physics is illustrated in Figure 8 which shows the size of flux uncertainties on the quasi-elastic cross section measurement. Error bars on points show the contributions to the flux uncertainty which arise from beamline component modeling at the current level of precision (from MINOS). The Outer band shows the combined total error from current production (pre MIPP) and beamline component modeling in quadrature. At

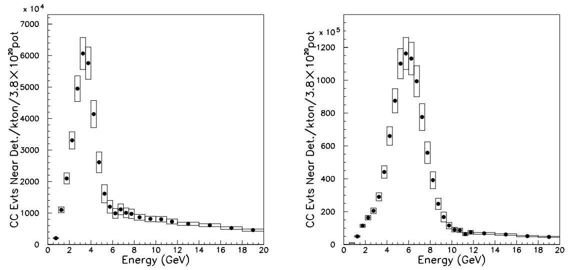

Figure 7: Uncertainties from modeling production and from beamline element optics (alignment, currents) in GNUMI from MINOS. The plots are LE beam (left) and sME beam (right). Note that the sME beam will not have the same uncertainties in the focusing peak as for the optimized ME beam.

the current level of precision flux uncertainty will dominate the QE cross section measurement in MINERνA and limit precision to $\sim$8-15% level.

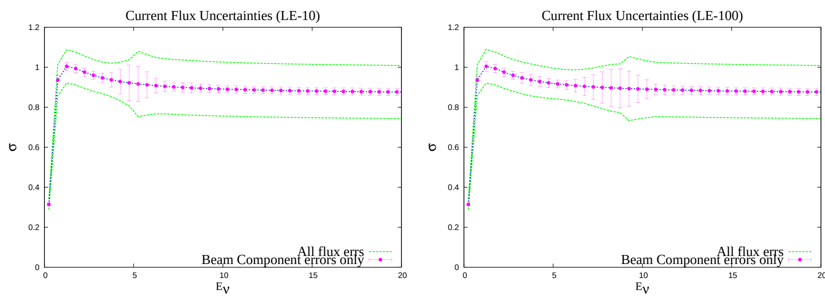

Figure 8: Uncertainties from knowledge of the flux. Error bars on points show the contributions to the flux uncertainty which arise from beamline component modeling at the current level of precision (from MINOS). Outer band shows the combined total error from current production (pre MIPP) and beamline component modeling in quadrature. The plots are LE beam (left) and sME beam (right).

Figure 9 shows the effect that MIPP projected uncertainties will have on the expected flux prediction. The plots assume that MIPP will reduce production uncertainties to the level of 4%. Beam component uncertainties will also change (the plots do not reflect this). After MIPP results are incorporated the flux prediction will be much improved and may be dominated by beamline component tolerances (alignment and current precision).

Figure 10 shows the effect of including flux errors on the measurement of the charged-current coherent cross section in MINERνA. The plot assumes all running is in the LE beam. The contribution from the flux uncertainty is comparable to the statistical precision for this measurement. Reducing the flux errors will make the coherent cross section measurements statistics limited.

References

[1] MINOS Collaboration, “MINOS Technical Design Report“, NuMI-NOTE-GEN-0337 (1998).

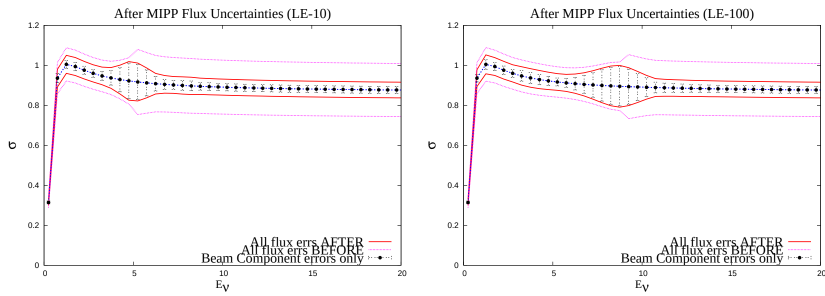

Figure 9: Estimate of flux uncertainties after MIPP data are incorporated into the flux prediction. Inner band (red) shows the total flux uncertainty assuming 4% production uncertainties (after MIPP) and beamline component uncertainties unchanged. The outer band (pink) shows the pre-MIPP total uncertainty band. Error bars on the points show the contribution to the flux uncertainty from beamline component tolerances (at the current level) only. The plots are LE beam (left) and sME beam (right).

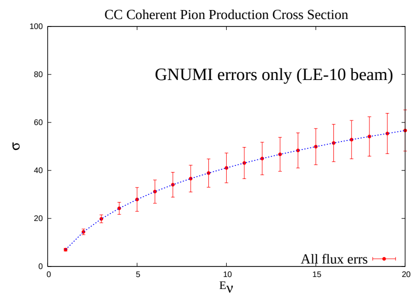

Figure 10: Size of contribution to uncertainty on the charged-current coherent cross section from flux uncertainties only (at the current level of precision pre-MIPP).

[2] N. V. Mokhov, "The MARS Monte Carlo", FERMILAB FN-628 (1995); N. V. Mokhov and O. E. Krivosheev, "MARS Code Status", FERMILAB-Conf-00/181 (20 00); http://www-ap.fnal.gov/MARS/.

[3] N. Mokhov and A. Van Ginneken, J. Nucl. Sci. Tech. **S1**, 172 (2000).

[4] M. Messier (private communication)

[5] Y. Hayato, To be published in *Proceedings of the Second Workshop on Neutrino-Nucleus Interactions in the Few-GeV Region (NUINT02)*, Irvine, California (2002).

[6] G. Ambrosini *et al.* [NA56/SPY Collaboration], Eur. Phys. J. C **10**, 605 (1999).

[7] P-907: Proposal to Measure Particle Production in the Meson Area Using Main Injector Primary and Secondary Beams, May 2000

`(http://ppd.fnal.gov/experiments/e907/Proposal/E907_Propsal.html)`

[8] NuMI Technical Design Handbook

(http://www-numi.fnal.gov/numiwork/tdh/tdh_index.html)

[9] K. Kodama *et al.*, Nucl. Phys. Proc. Suppl **98**, 43-47 (2001)

[10] M. Hasegawa *et al.* [K2K Collaboration], Phys. Rev. Lett. **95**, 252301 (2005) [arXiv:hep-ex/0506008].

[11] S. Kopp, Z. Pavlovic, and D. Indurthy, "Systematic Uncertainties in the NuMI Beam Flux" MINOS-doc-1283, (2006)

[12] C.H. Llewellyn Smith, Phys. Rep. 3C (1972).

[13] J. Arrington, nucl-ex[0305009].

[14] M. K. Jones *et al.*, Phys. Rev. Lett, 84, (2000) 1398 ; O. Gayou *et al.*, Phys. Rev. Lett, 88 (2002) 092301.

[15] J.J. Kelly, Phys. Rev. C70 (2004) 068202.

[16] R. Bradford, et al., hep[ex0602017].

[17] H. Budd, A. Bodek and J. Arrington, hep-ex[0308005].

[18] R. F. Wagenbrunn *et al.*, hep-ph[0212190].

[19] R. C. Merenyi *et al.*, Phys. Rev. D 45, 743 (1992)

[20] V. Bernard, L. Elouadrhiri, U.G. Meissner, J.Phys.G28 (2002), hep-ph[0107088].

[21] G. Zeller, private communication.

[22] K. Tsushima, Hungchong Kim, K. Saito, hep-ph[0307013].

[23] T. Kitagaki *et al.*, Phys. Rev. D26 (1983) 436.

[24] T. Kitagaki *et al.*, Phys. Rev. D42 (1990) 1331.

[25] S.J. Barish *et al.*, Phys. Rev. D16 (1977) 3103.
BNL D2

[26] N.J. Baker *et al.*, Phys. Rev. D23 (1981) 2499.

[27] W.A. Mann *et al.*, Phys. Rev. Lett. 31 (1973) 844.

[28] J. Brunner *et al.*, Z. Phys. C45 (1990) 551.

[29] M. Pohl *et al.*, Lett. Nuovo Cimento 26 (1979) 332.

[30] D. Allasia *et al.* Nucl. Phys. B **343** (1990) 285

[31] S.V. Belikov *et al.*, Z. Phys. A320 (1985) 625.

[32] S. Bonetti *et al.*, Nuovo Cimento 38 (1977) 260.

[33] K.L. Miller *et al.*, Phys. Rev. D26 (1982) 537.

[34] Glen Cowan, Statistical Data Analysis, Oxford Clarendon Press (1 998)

[35] H. Budd, A. Bodek and J. Arrington, hep-ex[0410055].

[36] D. Casper, Nucl. Phys. Proc. Suppl. 112 (2002) 161.

[37] R.A. Smith and E.J. Moniz, Nucl. Phys. B43 (1972) 605.

[38] Ghent Theory group in Belgium, Jan Ryckebusch (jan@inwpent5.UGent.be).

[39] D. Rein and L. M. Sehgal, Annals Phys. **133**, 79 (1981).

[40] M.H. Ahn, et al. (K2K), Submitted to PRD, hep-ex/0606032.

[41] T. Sato, D. Uno, and T.-S.H. Lee, Phys. Rev. C**67** 065201 (2003).

[42] E. Paschos, M. Sakuda, J.-Y. Yu, Phys. Rev. D**69** 014013 (2004).

[43] E. Paschos, et al., Proc. NuInt04 (L'Aquila), hep-ph/0408185.

[44] O. Lalakulich and E. Paschos, Phys. Rev. D**71** 074003 (2005).

[45] O. Lalakulich, E. Paschos, G. Piranishvili, Phys. Rev. D**74** 014009 (2006).

[46] T. Sato, et al., Proc. NuInt05 (Okayama),nucl-th/0601069.

[47] T. Kitagaki, et al., Phys. Rev. D**34** 2554 (1986).

[48] T. Kitagaki, et al., Phys. Rev. D**42** 1331 (1990).

[49] M. Hasegawa, et al. (K2K), Phys. Rev. Lett. **95** 252301 (2005).

[50] M. Wascko (MiniBoone), Proc. NuInt05 (Okayama), hep-ex/060 2050.

[51] D. Rein and L. M. Sehgal, Nucl. Phys. **B223**, 29 (1983).

[52] E. A. Paschos and A. V. Kartavtsev, (2003), hep-ph/0309148.

[53] Super-Kamiokande and K2K, C. Mauger, Nucl. Phys. Proc. Suppl. **112**, 146 (2002).

[54] BooNE, J. L. Raaf, Nucl. Phys. Proc. Suppl. **139**, 47 (2005), hep-ex/0408015.

[55] B. Z. Kopeliovich, Nucl. Phys. Proc. Suppl. **139**, 219 (2005), hep-ph/0409079.

[56] E. A. Paschos, A. Kartavtsev, and G. J. Gounaris, (2005), hep-ph/0512139.

[57] D. Rein and L. M. Sehgal, (2006), hep-ph/0606185.

[58] S. K. Singh, M. Sajjad Athar, and S. Ahmad, (2006), nucl-th/0601045.

[59] MiniBooNE, J. Monroe, Nucl. Phys. Proc. Suppl. **139**, 59 (2005), hep-ex/0408019.

[60] K2K, T. Ishida, Prepared for 1st Workshop on Neutrino - Nucleus Interactions in the Few GeV Region (NuInt01), Tsukuba, Japan, 13-16 Dec 2001.

[61] N.J. Baker *et al.*, Phys. Rev. D **24**, 2779 (1981).

[62] A. Alavi-Harati *et al.*, Phys. Rev. **87** 132001 (2001).

[63] P.G. Ratcliffe, Phys. Rev. **D59**, 014038 (1999).

[64] N. Cabibbo *et al.*, Semileptonic Hyperon Decay and CKM Unitarity, [arXiv:hep-ph/0307214] (July 2003).

[65] T. Alexopoulos *et al.* (KTeV Collaboration), Phys. Rev. Lett. **93**, 181802 (2004).

[66] T. Nakano *et al.*, [arXiv:hep-ex/0301020]; V.V. Barmin
em et al., [arXiv:hep-ex0304040]; S. Stepanyan [arXiv:hep-ex/0307018].

[67] R. Jaffe and F. Wilczek, Di-quarks and Exotic Spectroscopy, [arXiv:hep-ph/0307341] (July 2003).

[68] S. Kuhlmann *et al.*, Phys. Lett. B **476**, 291 (2000).

[69] H. Deden and et al., [Gargamelle Neutrino Collaboration], "Experimental Study Of Structure Functions And Sum Rules In Charge Changing Interactions Of Neutrinos And Anti-Neutrinos On Nucleons," Nucl. Phys. **B85**, 269 (1975).

[70] K. Varvell *et al.* [BEBC WA59 Collaboration], Z. Phys. C **36**, 1 (1987)

[71] M. Shifman, Handbook of QCD, Volume 3, 1451, World Scientific (2001)

[72] F. E. Close and N. Isgur, Phys. Lett. B **509**, 81 (2001)

[73] W. Melnitchouk, R. Ent and C. Keppel, Phys. Rept. **406**, 127 (2005) [arXiv:hep-ph/0501217].

[74] I. Niculescu *et al.*, Phys. Rev. Lett. **85**, 1186 (2000)

[75] C. E. Keppel, *Prepared for Exclusive Processes at High Momentum Transfer, Newport News, Virginia, 15-18 May 2002*

[76] J. Arrington, R. Ent, C. E. Keppel, J. Mammei and I. Niculescu, arXiv:nucl-ex/0307012 (submitted to Phys. Rev. Lett.)

[77] A. Fantoni [HERMES Collaboration], Eur. Phys. J. A **17**, 385 (2003).

[78] I. Niculescu *et al.*, Phys. Rev. Lett. **85**, 1182 (2000).

[79] A. Bodek and U. K. Yang, arXiv:hep-ex/0203009.

[80] D. Dolgov *et al.* [LHPC collaboration], Phys. Rev. D **66**, 034506 (2002) [arXiv:hep-lat/0201021].

[81] I. Niculescu, J. Arrington, R. Ent and C. E. Keppel, Phys. Rev. C **73**, 045206 (2006) [arXiv:hep-ph/0509241].

[82] X. Ji, Phys. Rev. Lett. **78**, 610 (1997).

[83] X. Ji, Phys. Rev. **D55**, 7114 (1997).

[84] A. V. Radyushkin, Phys. Lett. **B380**, 417 (1996).

[85] A. V. Radyushkin, Phys. Lett. **B385**, 333 (1996).

[86] J.C. Collins, L. Frankfurt, and M. Strikman, Phys. Rev. **D56**, 2982 (1997).

[87] A. V. Radyushkin, Nucl. Phys. **A711**, 99 (2002).

[88] M. Vanderhaeghen, Nucl. Phys. **A711**, 109 (2002).

[89] M. Diehl, hep-ph/0307382 (2003).

[90] C. Munoz Camacho, et al. nucl-ex/0607029 (2006).

[91] A. Psaker, W. Melnitchouk and A. Radyushkin, in preparation.

[92] D. Drakoulakos *et al.* [Minerva Collaboration], fine-grained detector in the NuMI beam," arXiv:hep-ex/0405002. Pgs. 99 - 108, 192 - 200.

[93] B.Z. Kopeliovich, hep-ph/0409079.

[94] M.K. Jones *et al.*, Phys. Rev. **C48**, 2800 (1993); R.D. Ransome *et al.*, Phys. Rev. **C46**, 273 (1992); R.D. Ransome *et al.*, Phys. Rev. **C45**, R509 (1992).

[95] D. Rowntree *et al.*, Phys. Rev. **C60**, 054610 (1999); B. Kotlinksi *et al.*, Eur. Phys. J. **A9**, 537 (2000).

[96] E. A. Paschos, M. Sakuda, I. Schienbein and J. Y. Yu, arXiv:hep-ph/0408185.

[97] M. Arneodo, Phys. Rept. **240**, 301 (1994).

[98] G. Piller and W. Weise, Phys. Rept. **330**, 1 (2000).

[99] B. L. Ioffe, V. A. Khoze, and L. N. Lipatov, *Hard processes: Phenomenology, Quark-Parton Model* (Elsevier Science Publishers, North Holland, 1984).

[100] G.B. West, Ann. Phys. **74** (1972) 464.

[101] S. V. Akulinichev, S. A. Kulagin, and G. M. Vagradov, Phys. Lett. B **158**, 485 (1985); S. V. Akulinichev, S. Shlomo, S. A. Kulagin, and G. M. Vagradov, Phys. Rev. Lett. **55**, 2239 (1985).

[102] S. A. Kulagin, Nucl. Phys. A **500**, 653 (1989).

[103] C. Ciofi degli Atti and S. Liuti, Phys. Rev. C **41**, 1100 (1990).

[104] F. Gross and S. Liuti, Phys. Rev. C **45**, 1374 (1992).

[105] S. A. Kulagin, G. Piller and W. Weise, Phys. Rev. C **50**, 1154 (1994).

[106] S. A. Kulagin, W. Melnitchouk, G. Piller, and W. Weise, Phys. Rev. C **52**, 932 (1995).

[107] S. A. Kulagin, Nucl. Phys. A **A 640**, 435 (1998).

[108] W. Melnitchouk, A. W. Schreiber and A. W. Thomas, Phys. Rev. D **49**, 1183 (1994).

[109] J. Gomez, *et al.,* Phys. Rev. D **49**, 4348 (1994).

[110] S. I. Alekhin, S. A. Kulagin and S. Liuti, Phys Rev. D **69**, 114009 (2004).

[111] S. A. Kulagin and R. Petti, paper in preparation.

[112] T. H. Bauer, R. D. Spital, D. R. Yennie and F. M. Pipkin, Rev. Mod. Phys. **50**, 261 (1978) [Erratum-ibid. **51**, 407 (1979)].

[113] C. A. Pickety, and L. Stodolsky, Nucl. Phys. B **15**, 571 (1970).

[114] S. L. Adler, Phys. Rev. **135**, B963 (1964).

[115] R. J. Glauber, Phys. Rev. **100**, 242 (1955).

[116] V. N. Gribov, Sov. Phys. JETP **29**, 483 (1970) [Zh. Eksp. Teor. Fiz. **56**, 892 (1969)] ; Sov. Phys. JETP **30**, 709 (1970) [Zh. Eksp. Teor. Fiz. **57**, 1306 (1969)].

[117] B. Z. Kopeliovich, and P. Marage, Int. J. Mod. Phys. A **8**, 1513 (1993).

[118] S. A. Kulagin, arXiv:hep-ph/9812532.

[119] E. A. Paschos and L. Wolfenstein, Phys. Rev. D **7**, 91 (1973).

[120] G. P. Zeller *et al.* [NuTeV Collaboration], Phys. Rev. Lett. **88**, 091802 (2002) [Erratum-ibid. **90**, 239902 (2003)] [arXiv:hep-ex/0110059].

[121] S. A. Kulagin, Phys. Rev. D **67**, 091301 (2003) [arXiv:hep-ph/0301045].

[122] S. A. Kulagin, arXiv:hep-ph/0406220.

[123] S. A. Kulagin, arXiv:hep-ph/0409057.

[124] D. H. Lu, A.W. Thomas, and K. Tsushima, arXiv:nucl- th/0112001, K. Tsushima, H. Kim, and K. Saito, Phys. Rev. C **70**, 038501 (2004)

[125] J.J. Aubert et al., Phys. Lett. **123B**, 275 (1983); D.F. Geesaman, K. Saito, and A.W. Thomas, Annu. Rev. Nucl. Part. Sci. **45**, 337 (1995).

[126] B. Buck and S.M. Perez, Phys. Rev. Lett. **50**, 1975 (1983).

[127] S. Dieterich, et al., Phys. Lett. B **500**, 47 (2001), S. Strauch et al., Phys. Rev. Lett. **91**, 052301 (2003).

[128] JLab experiment E3-104, co-spokespersons R. Ent, R. Ransome, S. Struach, P. Ulmer. `http://www.jlab.org/exp_prog/proposals/03/PR03-104.ps`

[129] C.H.Q. Ingram, Nucl. Phys. A **684**, 122 (2001).

[130] M. K. Jones *et al.*, Phys. Rev. C **48**, 2800 (1993).

[131] M. Nakahata *et al*, Nucl. Instrum. Meth. **A421**, 113 (1 999); E. Blaufuss *et al*, Nucl. Instrum. Meth. **A458** 638 (2001).

[132] M. Diwan and J. Nelson, NuMI-NOTE-STEEL-0639 (2000)

[133] PhD Thesis of C. Smith, University College London, London, 2002 *Calibration of the MINOS Detectors and Extraction of Neutrino Oscillation Parameters*; PhD Thesis of R. Nichol, University College London, London, 2003 *Calibration of the MINOS Detectors*

[134] PhD thesis of M. A. Kordosky, University of Texas at Austin, August 2004 *Hadronic Interactions in the MINOS Detectors*

[135] PhD thesis of P. L. Vahle, University of Texas at Austin, August 2004 *Electromagnetic Interactions in the MINOS Detectors*

[136] E. A. Paschos, L. Pasquali and J. Y. Yu, Nucl. Phys. B **588**, 263 (2000) and E. A. Paschos, J. Y. Yu and M. Sakuda [arXiv:hep-ph/0308130].

[137] D. Ashery *et al.*, Phys. Rev. **C23**, 2173 (1981).

[138] H. Gallagher, Nucl. Phys. Proc. Suppl. **112**, 188 (2002)

[139] NuMI Fluxes courtesy of Mark Messier

[140] The simulation assumed the active material was resistive plate chambers and the absorber was particle board (hydrocarbons).

[141] G.P.Zeller, submitted to proceedings of 2nd International Workshop on Neutrino - Nucleus Interactions in the Few GeV Region (NUINT 02), Irvine, California, 12-15 Dec 2002 [hep-ex/0312061]

[142] Kamiokande Collaboration, S. Hatakeyama *et al.*, Phys. Rev. Lett. **81** (1998) 2016; Soudan-2 Collaboration, W. W. Allison *et al*, Phys. Lett. **B 449** (1999) 137; MACRO Collaboration, Ambrosio *et al*, Phys. Lett. **B434**, 451 (1998)

[143] Y. Fukuda et al., *Phys. Rev. Lett.* **81** (1998) 1158; Erratum **81** (1998) 4279, B.T. Cleveland et al., *Astrophys. J.* **496** (1998) 505. W. Hampel et al. (GALLEX Collaboration), *Phys.Lett.* **B 447** (1999) 127., J.N. Abdurashitov et al. (SAGE Collaboration), *Phys. Rev.* **C 60** (1999) 055801 [astro-ph/9907113]

[144] Q.R. Ahmad *et al.* Phys.Rev.Lett.**89** (2002) 011302 nucl-ex/0204009

[145] Y. Fukuda *et al.*, Phys.Rev.Lett.**81** (1998) 1562 [hep-ex/9807003]; M. Sanchez et al., Phys. Rev. **D 68**, 113004 (2003)

[146] KamLAND Collaboration (K. Eguchi et al.), Phys. Rev. Lett.**90** (2003) 021802 [hep-ex/0212021]

[147] K2K Collaboration (M.H. Ahn et al.), Phys.Rev.Lett.**90** (2003) 41801 [hep-ex/0212007]

[148] B. Pontecorvo and J. Exptl, Theoret. Phys. **34** 247 (1958); Z. Maki, M. Nakagawa and S. Sakata, Prog. Theor. Phys. **28**, 870 (1962).

[149] M. Maltoni *et al*, submitted to New J. Phys, [hep-ph/0405172]

[150] By CHOOZ Collaboration (M. Apollonio et al.), Phys.Lett.**B466** (1999) 415 [hep-ex/9907037]

[151] W. Grimus and L. Lavoura, Phys. Lett. **B572**, 189 (2003); A. Aranda, C.D. Carone, R.F. Lebed, Phys. Rev. **D62**, 016009 (2000).

[152] "A Long Baseline Neutrino Oscillation Experiment at Fermilab", E.Ables *et al*, FERMILAB-PROPOSAL-0875, Feb. 1995, 241pp.

[153] "NOVA: Proposal to build an Off-Axis Detector to Study $\nu_\mu \to \nu_e$ oscillations in the NuMI Beamline", I. Ambats *et al.*, FERMILAB-PROPOSAL-0929, Mar 2004.

[154] Y. Itow *et al*, "The JHF-Kamioka Neutrino Project", KEK report 2001-4, June 2001. [hep-ex/0106019]

[155] J. Nelson, "MINOS Oscillation Results", Neutrino 2006, Santa Fe, NM, June, 2006.

bibitemingram C.H.Q. Ingram, Nucl. Phys. A **684**, 122 (2001).

[156] E. Gallas & J. Li., "Polishing Optical Fibers for the D0 ICD in Run II", FNAL-TM-2062, 1998.

[157] The MINERνA Collaboration,
Proposal to perform a high-statistics neutrino scattering experiment using a fine-grained detector in the NuMI beam, Fermilab Proposal P-938, e-print hep-ex/0405002; see Sect. 16.5.2.

[158] M. Bonkowski, *Magnetic Field Measurement Results*,
MINERνA note MINERvA-doc-88-v1, (measurements of December 2004).

[159] D. Cherdack and W.A. Mann, *Magnetic Shielding Capabilities of the MINERvA PMT Box*, MINERνA note MINERvA-doc-164-v1.

[160] P. Adamson, et al., Nucl. Inst. Meth. A**492**,
325 (2002).

[161] P. Shanahan, priv. comm. (Nov., 2005).

[162] A. Cabrera, et al., NuMI-934 internal report.

[163] P. Harris (Sussex Univ.) provided excellent
guidance and some pieces necessary for prototyping.

[164] "MCM II and the Trip Chip", J. Estrada, C. Garcia, B. Hoeneisen and P. Rubinov, August 2002, FERMILAB-TM-2226.

[165] MINOS Technical Design Report, Chapter 5: Scintillator detector fabrication, Fermilab Public

[166] Specification 9216.000-ES-435360. Available through the Fermilab Particle Physics Division.

[167] Specification 9216.000-ES-435361. Available through the Fermilab Particle Physics Division.

[168] R. Bradford, *Assembly Roadmap from Prototype Studies*, posted to FNAL MINERνA Docdb as document number 561.

[169] R. Flight, *Detector Assembly Drawings, as of 11/15/05*, available in MINERνA Docdb as document number 226.

[170] R. Flight, *Mapper Drawings*, available in MINERνA Docdb as document number 897.

[171] R. Flight, *Fiber Routing Update*, available in MINERνA Docdb as document number 741.

[172] D. Casper, "The nuance Neutrino Physics Simulation, and the Future", *http://nuint.ps.uci.edu/nuance/files/nuance_nuint01.pdf*

[173] O. Benhar, [arXiv:nucl-th/0307061].

[174] K. Ruddick (private communication).

[175] L. Mualem (private communication).

[176] MINOS Collaboration, P. Adamson *et al.*, IEEE Trans. Nucl. Sci. **49**, 861 (2002).

[177] R. Fruhwirth, Nucl. Inst. Meth. **A262**, 444 (1987).

[178] "Studies of Extruded Plastic Scintillator for MINOS", Karol Lang and Todd Soesby, NuMI-NOTE-L-250, Feb 1997.

[179] M. Andrews, MINERνA Hazard Assessment, MINERνA Document 310 (2006)

[180] MINERνA Project Management Plan, MINERνA Document 59 (2006)

[181] L. Mualem, *The case for using Cesium-137 on the module mapper instead of Co-60*, NuMI-L-0653 (2000)

[182] American Institute of Steel Construction, Inc., *Manual of Steel Construction, Allowable Stress Design*, Ninth Edition

[183] American National Standard ANSI/ASME B30.20, *Below-the-hook lifting devices*

[184] Gage-Babcock & Associates, Inc. *Fire Protection/Life Safety Recommendations for the Fermilab NuMI Project* (1998)

[185] Fermilab ES&H Manual, Chapter 5032.2, Guidelines for the Design, Review and Approval of Liquid Cryogenic Targets (1995)

[186] J. Livengood, Letter to G. Brown, *National Environmental Policy Act (NEPA) Determination at Fermi National Accelerator Laboratory - "Main Injector Neutrino ExpeRiment ν–A(MINERνA)"* MINERνA Document 311 (December 2, 2005)